Renewable Energy 83 (2015) 1287–1298

Contents lists available at ScienceDirect

Renewable Energy

journal homepage: www.elsevier.com/locate/renene

Review

Aggregated models of permanent magnet synchronous generators wind farms

M.J. Mercado-Vargas*, D. Gómez-Lorente, O. Rabaza, E. Alameda-Hernandez

Department of Civil Engineering, Section of Electrical Engineering, University of Granada, Spain

ARTICLE INFO

Article history:
Received 14 March 2014
Accepted 16 April 2015
Available online 13 May 2015

Keywords:
Permanent magnet synchronous generator
Aggregated wind farm model
Equivalent wind method
Approximate mechanical torque method
Equivalent wind turbine rotor method

ABSTRACT

This paper evaluates the responses of three aggregated models of a wind farm consisting of variable speed permanent magnet synchronous generator wind turbines when wind fluctuations or grid disturbances occur. These responses are compared with those of the detailed wind farm model, in order to verify the effectiveness of the studied aggregation methods for this type of wind farms. The equivalent wind farm models have been developed by adapting different aggregation criteria that already exist in technical literature and had been applied to other technologies. In this work, these methods have been modified to suit them to the permanent magnet synchronous generator technology. The results show that the three aggregated models provide very similar results to the detailed model, both in the evolution of active power when fluctuations in wind speed occur, and in the active power and DC-link voltage during the two simulated voltage dips. Notably, the aggregated model with an approximate mechanical torque offers excellent results.

1. Introduction

Interest in wind energy continues experiencing a progressive growth worldwide due to lower generating costs, an increase in electricity demand and a rising concern for the environment. In fact, the worldwide wind capacity reached close to 300 GW by the end of June 2013 and all wind turbines globally installed by mid-2013 can generate around 3.5% of the world's electricity demand [1]. In particular, according to last data published by *Red Eléctrica de España (REE)*, in 2013 wind energy has been the technology that has contributed more to cover the annual electricity demand in Spain for the first time, with a 21.3%, being located a little above the nuclear which has achieved a 21% contribution [2]. Consequently, nowadays wind energy is a real alternative to conventional energy what allows diversification of energy sources and reduces the dependence on imports.

Penetration of wind energy in the power system is huge so that, the performance of the power system depends on the behaviour of its main characters. This performance is supervised by the system operator, who needs to know beforehand the behaviour of all constituents, in particular, all the generation units, like wind farms. On the order hand, in order to get the maximum of renewable resources, it is a common practice not to restrict wind generation.

Hence, it is for these reasons that there is a need for developing wind farm (WF) models that represent the collective reaction of wind turbines (WTs) to grid disturbances and different wind conditions. But this task is computationally very demanding due to the size of WFs, which keeps increasing. Therefore, when the entire WF is simulated by representing each individual turbine, the response simulation time is very slow because of the complexity of the system of equations that describes it. Then, to study the behaviour of one or more WFs within the power system in transient stability studies, it is common to represent the whole WF by groups of turbines or by one single equivalent turbine, what is known as an *equivalent or aggregate model* of the WF. Thereby, the complexity of the system and the calculation time are reduced without losing information on the WTs collective response.

Equivalent models by adding variable speed WTs are only being studied since a few years ago and most of the investigations are focused on WFs with doubly fed induction generators (DFIG) WTs [3], [4]. However, this configuration is being gradually replaced by

Abbreviations: WF, wind farm; WT, wind turbine; DFIG, doubly fed induction generator; PMSG, permanent magnet synchronous generator; EWT, equivalent wind turbine; SCIG, squirrel cage induction generator; AWF, aggregate wind farm.

* Corresponding author. Department of Civil Engineering, E.T.S.I.C.C.P., Campus of Fuentenueva s/n., University of Granada, 18071, Granada, Spain. Tel.: +34 958 241000x20448; fax (+34) 958 246138.
E-mail address: mjmercado@ugr.es (M.J. Mercado-Vargas).

http://dx.doi.org/10.1016/j.renene.2015.04.040
0960-1481/

the permanent magnet synchronous generator (PMSG) WT, which is becoming the most used configuration by most manufacturers, due its attractive characteristics versus other configurations [5]. Therefore, there is a need to carry out aggregated models by adding variable speed PMSG WTs and, nevertheless, there is evidence in the literature that such models of WFs have hardly been developed.

After analyzing the state of the art of aggregate models of WFs with variable speed wind turbines, it can be pointed out that to represent a variable speed WF behaviour in the presence of wind fluctuations or grid disturbances, basically, there are two aggregation methods. However, each author adapts these aggregation methods to his targets and changes the level of reduction depending on the type of the study to be performed, the wind distribution within the WF and the level of accuracy required.

The first main aggregation method is the simplest and most used one and it is based on the aggregation of a whole WF into a single equivalent WT. The mechanical and electrical parameters of the equivalent wind turbine (EWT) are scaled properly and its rated power is the sum of the nominal power of each WT within the WF [3,6,7]. In this aggregation method it is assumed that all WTs within the WF are receiving the same wind and, therefore, all the machines are producing the same electrical power. However, although the order of the WF model can be highly reduced and, in consequence, the simulation time, the WF generating capacity is overestimated when this aggregation method is used, since the variation of wind speed within the WF due to its layout has not been taken into account and, therefore, the result is not accurate enough. So a single equivalent machine with a uniform wind speed distribution is not a good solution to represent the behaviour of a whole WF [8].

This problem can be solved with a variation in the described aggregation method: grouping together the WTs with similar incoming wind speeds within a WF and replacing them by an EWT. Then, the aggregate WF model will have so many EWTs as groups of machines with identical wind conditions [3,9]. The results of this method are more accurate but, as there are many WFs with different wind speed conditions within it, the resulting equivalent model may need many EWTs to represent the WF, which can result in long simulation time [8].

In Refs. [4,10] are presented variations of the one-machine aggregate model. In Ref. [10] the EWT receives an equivalent incoming wind, which is derived from the power curve and the wind experienced by each WT, being identical all of them. Although this method allows a reduction of the equivalent model order, its main disadvantage is that different WTs can not be aggregated because the equivalent system power curve can not be estimated. In Ref. [4], the proposed aggregation method results in an EWT where the mechanical systems of WTs are also aggregated. This method allows a whole WF to be represented at PCC to grid even when different wind turbines are operating with different incoming winds.

The second main aggregation method to represent a variable speed wind farm behaviour in the presence of wind fluctuations or grid disturbances is based on aggregating just the electrical system and modelling the mechanical system of each individual WT in order to consider the different wind speed conditions within the WF and even different technologies [11,12].

In Ref. [12] a dynamic simplified model of each individual WT is used to approximate their operation points according to the incoming wind. Then, the generator mechanical torque of the individual WTs are aggregated and the resulting torque is applied to the equivalent generator system. The results obtained with this aggregation method are more accurate than the ones obtained from the single equivalent machine or its variations, but some authors consider that the number of differential equations required to model the dynamic simplified WT is still reasonably large [8].

These aggregation methods can be summed up as shown in Table 1.

As aforementioned, despite the boom experienced by the PMSG WTs in the last few years, aggregated models of WFs with PMSG WTs barely exist in technical literature. For this reason, in this paper three aggregation methods from the summarised in Table 1 have been used to develop three equivalent models of WFs with variable speed PMSG WTs to study dynamic power systems. The most extended methods are analysed in this work:

- Method 1-Variation 2, which is named in this work *equivalent wind method*, is first proposed in Ref. [10] for squirrel cage induction generator (SCIG) and DFIG WTs.
- Method 1-Variation 3, which is named in this work *equivalent wind turbine rotor method*, is first proposed in Ref. [4] for variable speed DFIG WTs.
- Method 2, which is named in this work *approximate mechanical torque method*.

The procedure used to validate the developed equivalent models against the detailed WF model is based on the method proposed by the Working Group 21 of the IEA Wind [13] for variable speed DFIG WFs, adapting some of these requirements to the WTs that are studied in this work, to the best of the author knowledge.

The paper is organized as follows: Section 2 describes the detailed adopted model of the PMSG WT and its control system; Section 3 explains the aggregation methods used, Section 4 evaluates and discusses the responses of the equivalent models of the studied WF when wind fluctuations or grid disturbances occur and, finally, Section 5 presents the conclusions extracted from this research.

The software used for simulations is MATLAB/Simulink.

2. Detailed adopted model of a wind turbine

2.1. Wind turbine configuration

A typical configuration of a PMSG WT is shown in Fig. 1 and the equations that define the models of the different WTs components are given in Appendix A. These equations have already been described in Refs. [14,15], according to widely used PMSG WT models in the literature [16,17].

2.2. Wind turbine control system

The wind turbine consists of two coordinate control systems: the frequency converter control system and the blade pitch angle one. The WT control system used in this paper is already described in Ref. [15].

Depending on the objectives sought by each author, different control strategies are used in the generator-side converter control systems: Rotor speed control strategy (getting the reference of the generator-side converter from the measured wind speed [18–20] or from the measured electrical power [21]), electrical torque control strategy [22,23] and power control strategy [17,18,24,25]. In this work, the power control strategy has been adopted because in presence of a wind fluctuation this control strategy provides a smoother behaviour, although the WT system takes longer to restore the steady-state. Hence the WTs components are less stressed and the risk of structural damages to the WT components is lower [15,26]. Fig. 2 shows the schemes of the generator-side and the grid-side converter control systems.

On the other hand, regarding the pitch angle control system, as power control is the strategy applied to the outer loop of the generator-side converter control system and since it is a speed

Table 1
Aggregation methods.

Name	Characteristics	Advantages	Disadvantages
Method 1	EWT presents rescaled power capacity. All WTs within the WF receive the same wind.	The WF model order and the simulation time are highly reduced.	Overestimated WF generation capacity due to not considering the wind speed variation within the WF.
Variation 1	WTs with similar incoming winds are grouped and replaced by an EWT. The aggregate WF model will have as many EWTs as groups of machines with identical wind speed conditions.	More accurate results.	Long time simulation.
Variation 2	EWT receives an equivalent incoming wind, which is derived from the power curve and the wind experienced by each WT.	Good results and high reduction of the order model.	If WTs within the WF are different, they can not be aggregated because it is not possible to get the equivalent system power curve.
Variation 3	The mechanical system of the WTs are aggregated and the EWT also receives an equivalent incoming wind.	Good results and high reduction of the order model.	
Method 2	The mechanical system of each WT is modelled separately in order to approximate their mechanical torque. The resulting torque is applied to the equivalent electrical system	Very good results.	The WF model order is still large.

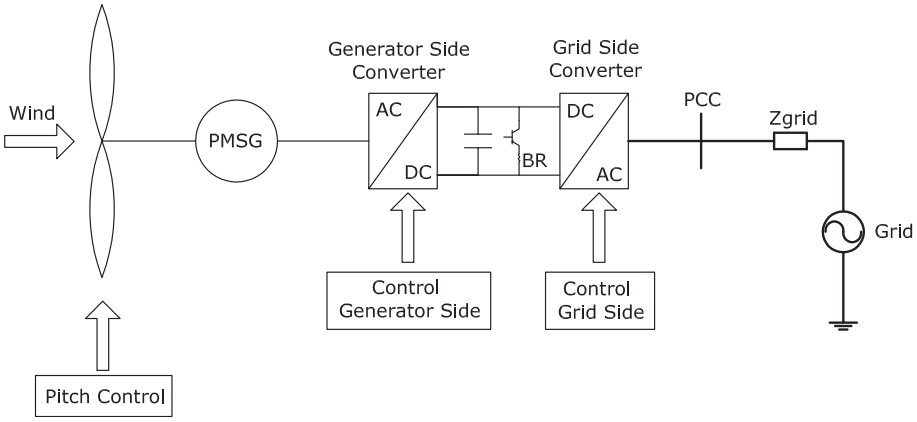

Fig. 1. Block diagram of a wind turbine based on PMSG.

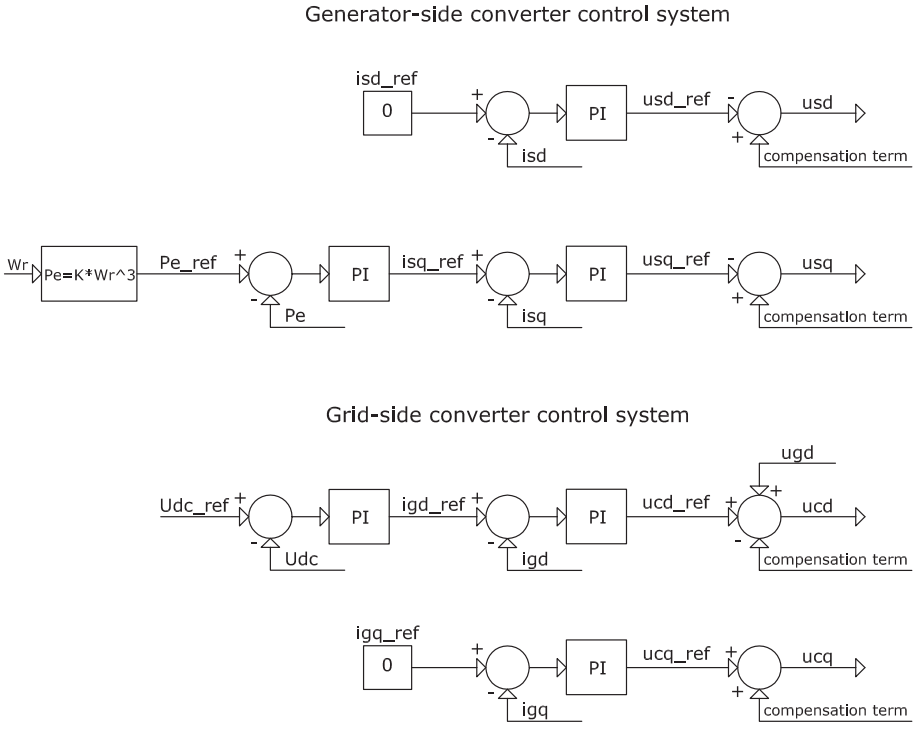

Fig. 2. Generator-side and grid-side converter control system schemes.

indirect control strategy [27], the pitch angle control system has been implemented to regulate the wind rotor speed [15], as shown in Fig. 3.

3. Equivalent models of wind farms with PMSG wind turbines

Knowing the detailed model of the PMSG WT and, in consequence, the detailed model of the studied WF, three aggregated wind farm (AWF) models have been developed by applying different aggregation criteria that already exist in technical literature and have been applied to other technologies. In this work, these methods have been modified to suit them to the PMSG technology, described next.

3.1. Equivalent wind method

This aggregation method can be found in Refs. [4,10] for SCIG and DFIG WTs. It proposes the aggregation of all WTs of a WF in a single equivalent machine that has re-scaled power capacity and receives an equivalent incoming wind, derived from the power curve and the wind experienced by each WT within the WF.

As mentioned in Ref. [4], this aggregation method is suitable for any kind of WT regardless of the incident wind; so that it can be applied to a WF with PMSG WTs without requiring any changes. To apply this aggregation method to the studied WF, the following suppositions have been done:

- An approximation of the mechanical power generated by each WT is obtained from the power curve of each WT according to the incoming wind. In order to get the maximum power at each wind speed, it has been consider that all WT operate at optimum C_p [28]. The individual mechanical powers are added and the resulting one is the equivalent power. The equivalent wind is obtained from the equivalent power curve, obtained re-scaling the individual one, and the equivalent power, as shown in Fig. 4.
- The equivalent wind is used with the rotor model of an individual WT in order to calculate its mechanical torque. As all the aggregated WTs within the WF receive the equivalent wind, all of them produce the same mechanical torque and, therefore, the equivalent rated mechanical torque is N times the rated mechanical torque of the individual WTs, where N is the number of aggregated WTs.
- The equivalent drive train is represented by the one mass model [15,16] because the shaft dynamics are neglected since in variable speed WTs the shaft properties are hardly reflected at the grid connection due to the decoupling effect of the power converter. The equivalent system inertia is N times the inertia of the individual WT. Whereas in Ref. [10], the drive train of the EWT is the one of an individual WT, which is represented by the two mass model.
- The equivalent generation system is composed of the third order model of a PMSG and an equivalent converter.
- The control system of the EWT keeps the same model of the individual WTs but the control parameters have been retuned.
- Unlike [10], it is assumed that each individual WT operates at unity power factor and, therefore, the reactive power of the EWT is zero.

In Fig. 5 the EWT diagram used in this method is depicted.

If the WTs within the WF are different, they can not be aggregated because it is not possible to get the equivalent system power curve. Then, to solve this problem, it is needed to develop an EWT model for each group of identical WTs [4].

3.2. Approximate mechanical torque method

The approximate mechanical torque method can be found in Refs. [4,12], for DFIG WTs and it proposes the aggregation of all WTs of a WF in a single equivalent machine to represent the whole WF at PCC to grid, even when WTs operate with different incoming winds. The EWT model includes an aggregated model of the generation systems and a dynamic simplified model of each individual WT to approximate their operation points according to the corresponding incoming wind speed.

In this work, to apply this aggregation method to the studied WF, the following suppositions have been assumed:

- The dynamic simplified model of each WT is composed of the rotor model, the drive train model, the PMSG represented by the mechanical equation, the rotor speed controller and the blade pitch angle controller, as depicted in Fig. 6.
- The equivalent mechanical torque is the sum of the individual mechanical torques, which are obtained from the simplified model of each WT and the incoming wind.
- The equivalent drive train is the same as in Section 3.1, while in Refs. [4,12] it is represented by the two mass model.
- The equivalent generation system and the control system of the EWT are the same as in Section 3.1.
- Unlike [4,12], each individual WT operates at unity power factor and, therefore, the reactive power of the EWT is zero.

Fig. 7 depicts the AWF model scheme according to the *approximate mechanical torque* method.

3.3. Equivalent wind turbine rotor method

This aggregation method also proposes the aggregation of all WTs of a WF in a single equivalent machine, which receives an equivalent incoming wind, to represent a whole WF at PCC to grid even when the WTs are different or identical machines operating with different incoming winds. This method was first proposed in Ref. [4] for variable speed DFIG WTs.

The *equivalent wind turbine rotor* method is a step beyond the *equivalent wind* aggregation method since, in this case, the mechanical systems of WTs are aggregated too. Therefore, it is assumed that being connected all WTs to the same internal WF network and being high power machines, the natural mechanical frequency will be similar and so the mechanical systems can be aggregated into an equivalent one that provides a response as close as possible to that of the individual WTs [4].

In order to apply this aggregation method to the studied WF, the assumptions done are mentioned next:

- The equivalent incoming wind is calculated as described in Section 3.1. However, in this case, the equivalent power curve is defined by the following expression [4]:

$$P_{m-eq} = \frac{1}{2}\cdot\rho\cdot A_{eq}\cdot C_{p-eq}\cdot V_{v-eq}^{3} \tag{1}$$

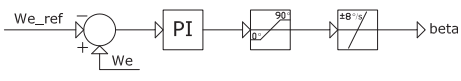

Fig. 3. Pitch angle control strategies.

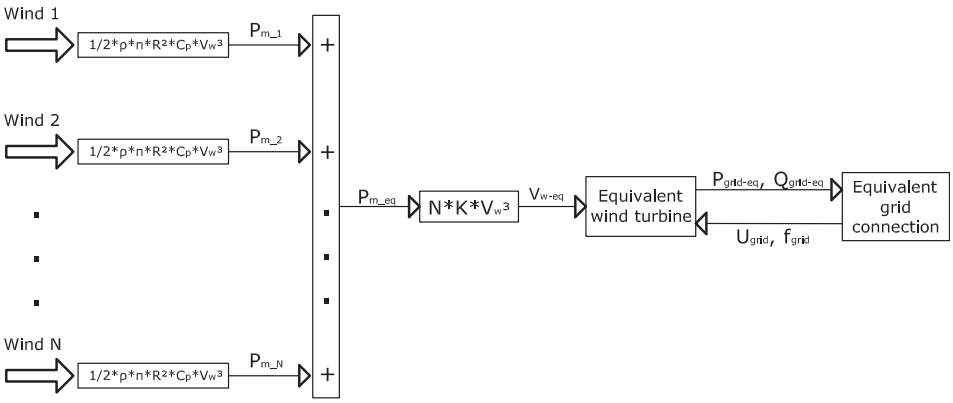

Fig. 4. Block diagram of the aggregated wind farm model according to the equivalent wind method.

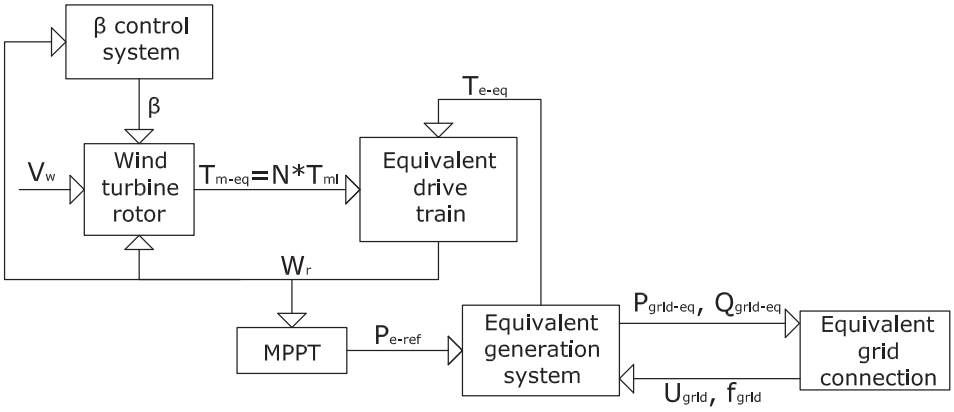

Fig. 5. Block diagram of the equivalent wind turbine uses in the equivalent wind turbine model.

where P_{m-eq} is the mechanical power developed by the EWT (W), A_{eq} is the area of the EWT, C_{p-eq} is the power coefficient of the EWT and V_{v-eq} is the incident equivalent wind speed (m/s).

This consideration allows different WTs to be aggregated, what means a high order model reduction.

- The equivalent area, A_{eq}, is obtained by considering that the EWT radius is the sum of the aggregated WTs radii [4], while the equivalent power coefficient, C_{P-eq}, is considered to be the same for all WTs at theirs optimum value, since calculations are simplified without making an excessive error.

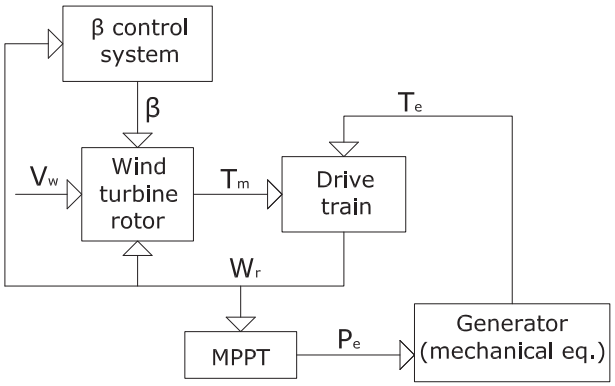

Fig. 6. Block diagram of the simplified wind turbine model used in the approximate mechanical torque method.

- The equivalent drive train is again represented by the one mass model but in this case the equivalent system inertia has been calculated from the following equation [29]:

$$H = \frac{\frac{1}{2}\cdot J'_{eq}\cdot W_r^2}{P_N}, \tag{2}$$

where H is the system inertia (s), J_{eq}' is the inertia of the aggregated WT (Kg m^2), W_r is the rotor speed (rad/s) and P_N (W) is the rated power of the EWT.

In Ref. [4], the equivalent drive train is represented by the two mass model.

- The equivalent generation system and the control system of the EWT are the same as in Section 3.1.
- As in Sections 3.1 and 3.2, the reactive power of the EWT is zero.

Fig. 8 shows the AWF model diagram according to the *equivalent wind turbine rotor* method.

4. Simulation results

The studied wind farm has a radial structure and consists of six variable speed PMSG WTs of 5 MW each one. WTs are connected to the internal electrical grid through a MV line at 3 kV and a common MV line connects the group of WTs to the WF substation, which presents a transformer 66/3 kV coupling the WF at 66 kV to grid, as Fig. 9 depicts.

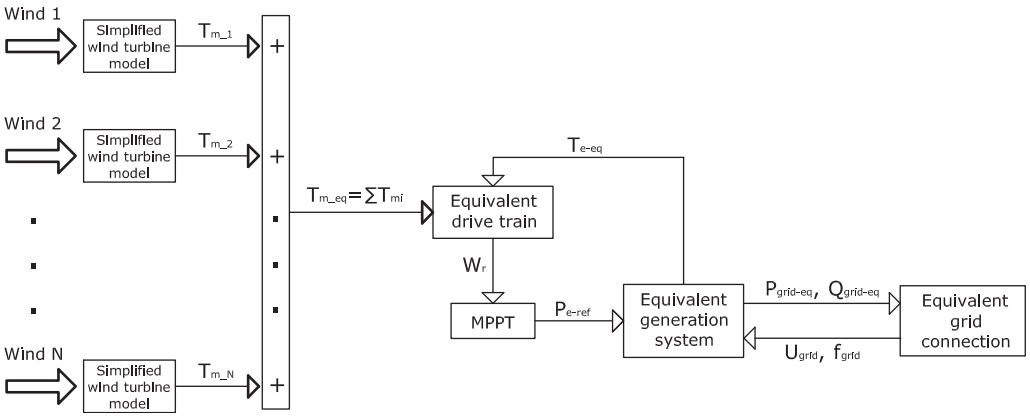

Fig. 7. Block diagram of the AWF model according to the approximate mechanical torque method.

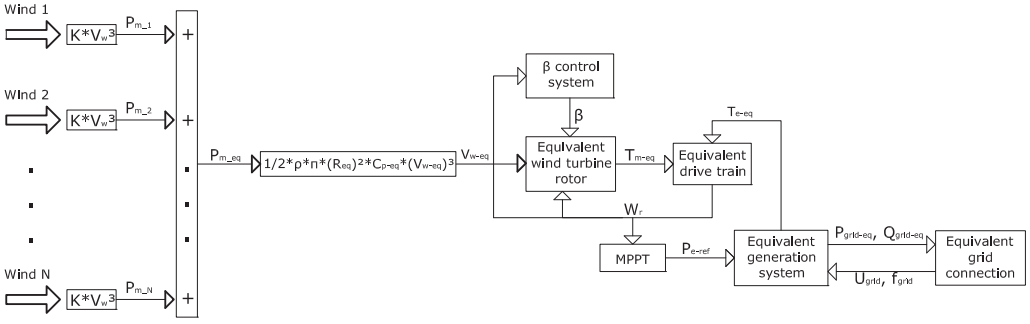

Fig. 8. Block diagram of the AWF model according to the equivalent wind turbine rotor method.

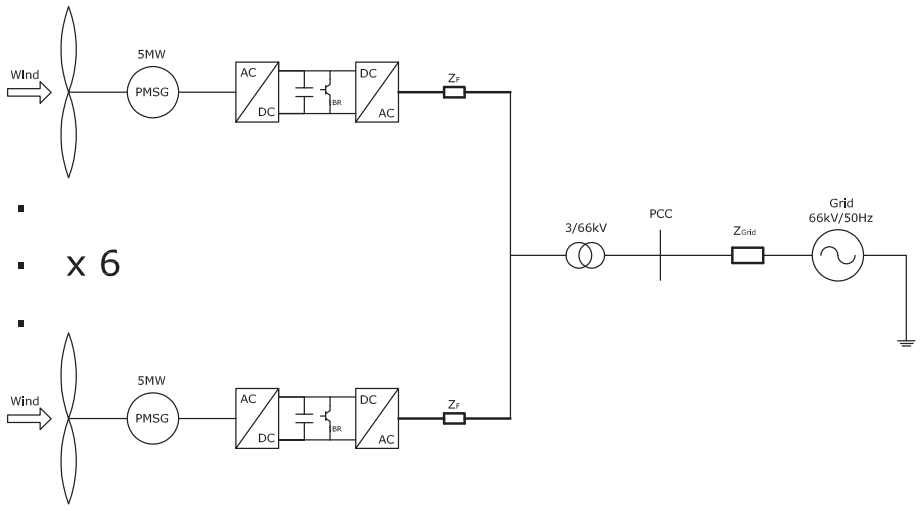

Fig. 9. Scheme of the studied wind farm.

The wind turbines and wind farm parameters are defined in Appendix B.

It has been considered that the WTs within the studied WF are placed in a row along a hill and widely separated, since this is a typical Spanish WF configuration. Therefore, the wake effect has not been taken into account because there are not WTs in the downwind direction, and in the crosswind direction the separation between them is long enough to disregard this effect [30]. Besides, it is considered that all WTs receive different incoming winds since they are located in a rough land and they are widely separated.

On the other hand, it has been assumed that the smoothing effect in the power fluctuation of the WF is negligible due to the studied WF is only composed of six wind turbines and they are spread over an area smaller than 10 km^2 [31].

The procedure used to validate the effectiveness of the developed AWF models to reproduce the studied WF response in the presence of wind fluctuations or grid disturbances is based on the method proposed by the Working Group 21 of the IEA Wind for variable speed DFIG WFs [13]. Time series of wind speed are introduced in the AWF models, getting to the output time series of

active power, reactive power and, optionally, voltage at PCC, when the responses to wind fluctuations are studied, and time series of active power and DC-link voltage to analyse the behaviour of the power converter during grid disturbances.

4.1. Time series of wind speed

In order to check the AWF models, two different tests have been performed. Each test consists of six time series of wind speed, one for each individual WT of the studied WF. These time series represent the different conditions to which a WF can be subjected during normal operation and have been developed from the wind model proposed in Ref. [32].

In this paper, the developed time series of wind speed only take into account the initial average value of the wind speed V_a and the component that represent the wind speed turbulence (defined by the turbulence length scale, l, the WT hub height h, the roughness length z_0, the frequency Δf and the number of sine functions with different frequencies N) as shown in Tables 2 and 3.

The initial average values of each one of the series have been selected according to the purpose of each test, as discussed below. Although the values of the parameters that define the wind turbulence are equal for both tests, turbulences depend on the initial values of wind speed; therefore, by adding the time components that represent the wind speed turbulence and the initial average values of wind speed for each one of the tests performed, different time series are obtained.

As an illustration, Fig. 10 shows the time series of wind speed for test 1. The initial average values of wind speed vary between 9 and 10.5 m/s, being these values below the rated wind speed, and therefore the objective of this test is to check the WF behaviour when it is operating below nominal conditions.

In the time series of wind speed for test 2, the initial average values of wind speed vary between 11.5 and 13 m/s. Since these values are above the rated wind speed, the objective of this test is to verify the WF behaviour when it is operating at nominal conditions.

4.2. Responses to wind fluctuations

Once the aggregation methods studied in this work have been described, it is necessary to check the developed equivalent models dynamic performances and compare the results with the detailed WF model behaviour.

This section shows the responses of the developed AWF models compared to the detailed WF model response after the performed tests. Next, to check the accuracy of the responses, the average distance between them is measured, being defined by the following equation [15]:

$$d_t = \left| \frac{\sum_{i=1}^{n} (X_1 - X_2)^2}{n \cdot X_1} \right| \cdot 100, \tag{3}$$

where d_t is the average distance (%), X_1 is the value of the considered variable in the detailed model response, X_2 is the value of the considered variable in the AWF model response and n is the number of considered points.

Table 2
Initial average wind speed values of tests 1 y 2.

V_a (m/s)						
Wind turbine	1	2	3	4	5	6
Test 1	9	9.4	9.8	10	10.2	10.5
Test 2	11.5	11.8	12	12.2	12.5	13

Table 3
Values of the parameters that define the wind turbulence for each test.

Parameters					
Test type	l (m)	h (m)	z_0 (m)	Δf (Hz)	N
Test 1	600	80	0.005	0.2	50
Test 2	600	80	0.005	0.2	50

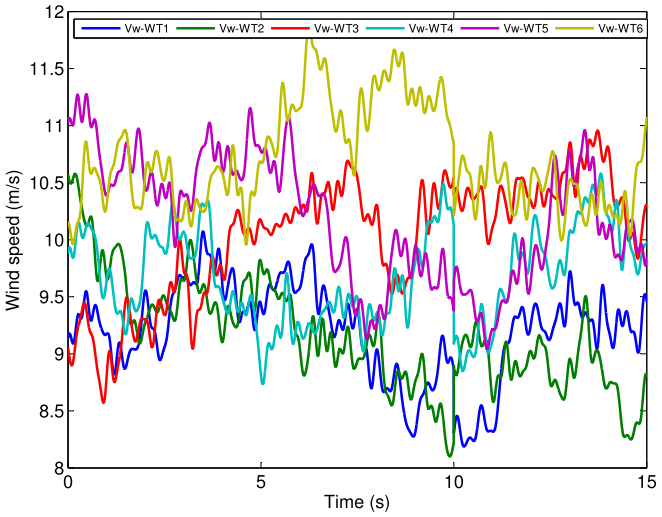

Fig. 10. Time series of wind speed for test 1.

Fig. 11 shows the time series of active power at PCC from the developed AWF models and the detailed one when the time series of wind speed for test 1 are introduced in the AWF models. As it can be seen in the figure, when the WF operates below nominal conditions, the three aggregation methods responses are virtually identical to the detailed model one.

The closeness of the results from the three developed AWF model is due to the advantage of adding identical machines. In the case of the AWF model according to the *equivalent wind turbine*

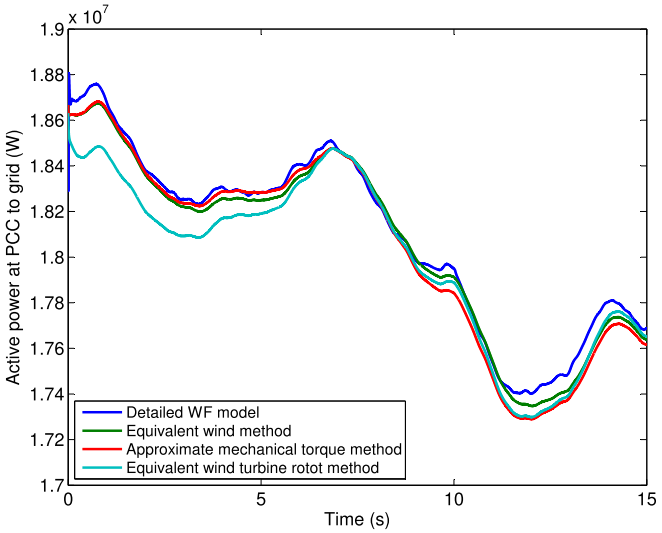

Fig. 11. Comparison of active power at PCC to grid generated by the detailed model and the three developed equivalent models during test 1.

Table 4
Comparison of the distance between the AWF models and the detailed model during test 1.

Average distance in active power delivered to the grid series (test 1) (%)		
Equiv. wind	Approx. T_m	EWT rotor
0.003	0.005	0.016

Table 5
Comparison of the distance between the AWF models and the detailed model in test 2.

Average distance in active power delivered to the grid series (test 2) (%)		
Equiv. wind	Approx. T_m	EWT rotor
0.763	0.010	0.755

rotor method, in addition to aggregating the electrical systems as in the other two AWF models, also the mechanical system is added and, therefore, the equivalent inertia of the machine is far greater than the inertia of the individual machines, causing a slow-down in response.

These similarities between the results of the AWF models with respect to that of the detailed model are confirmed by checking the total distances values. As can be seen in Table 4, the average distances between the AWF models according to the *equivalent wind* and the *approximate mechanical torque* methods and the detailed model is less than 0.01% in both cases, existing only a slight difference between the value of the average distance from the AWF model according to the *equivalent wind turbine rotor* method and the detailed model (0.02%). Therefore, it is clear that the three aggregation methods provide very good responses.

Results for test 2 are shown in Fig. 12. As the figure depicts, when the WF operates at nominal conditions, the responses of the AWF models according to the *equivalent wind* and the *equivalent wind turbine rotor* methods are displaced with respect to the detailed model one, being the response of the AWF model with *approximate mechanical torque* method virtually identical to the detailed model one.

The difference between the results is caused by the blade pitch angle control system. The *approximate mechanical torque* method uses a simplified model of each individual WT to achieve an approximate mechanical torque developed by each of them, so that the sum of them all, the equivalent mechanical torque, is the input of the EWT. Therefore, firstly the individual torques are calculated, which are affected by the action of the β control system corresponding to each of the machines, and afterwards the resulting mechanical torque is applied to the equivalent electrical system. However, in the case of the AWF models according to the *equivalent wind* and the *equivalent wind turbine rotor* methods, to calculate the incoming equivalent wind of the EWTs, C_p is considered optimum, without falling into a relevant mistake, so that, the blade pitch angle control system performance only affects the incoming winds of the EWTs but not the entries of these two aggregation methods.

Table 6
Comparison of time reductions for the studied aggregation methods in test 1 and test 2.

Simulation time	Test 1 (s)	Reduction (%)	Test 2 (s)	Reduction (%)
Detailed model	695.2185		711.8950	
EW method	584.0536	16	599.9272	**15.73**
AMT method	623.9871	10.25	614.7717	13.64
EWT method	575.9579	**17.15**	601.5311	15.50

Figures in bold show the best time reduction for wind fluctuation tests.

Again, the values of the average distance between the AWF models responses and the detailed model one verify that the three aggregation methods generate optimal results, as shown in Table 5, with the best model being the *approximate mechanical torque* method, with a distance value of 0.01%.

On the other hand, regarding the simulation time, as shown in Table 6, the best time reduction is about 17% for the *equivalent wind turbine rotor* method with respect to the detailed model in test 1, being the best time reduction in test 2 about 16% for the *equivalent wind* method with respect to the detailed model.

In this work it is assumed that the studied WF operates at unity power factor and, therefore, it was not considered necessary to get to the output time series of reactive power.

4.3. Response to grid disturbances

It is essential that wind systems be able to continue operating during transient disturbances in the network to ensure continuity of energy supply to all users. For this reason, most countries' system

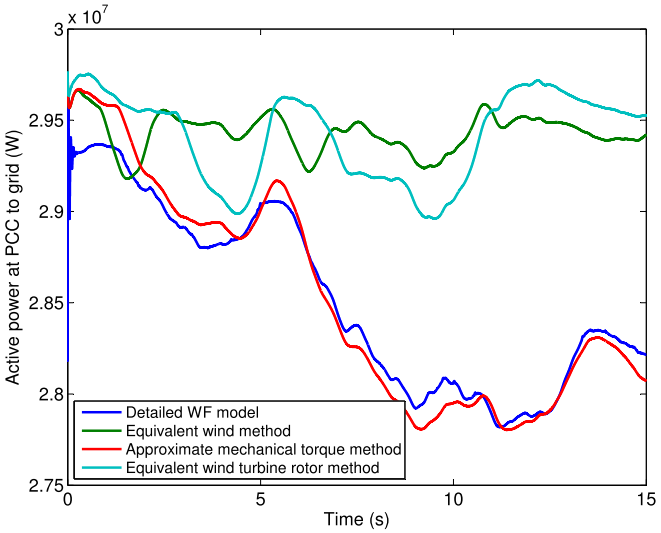

Fig. 12. Comparison of active power at PCC to grid generated by the detailed model and the three developed equivalent models during test 2.

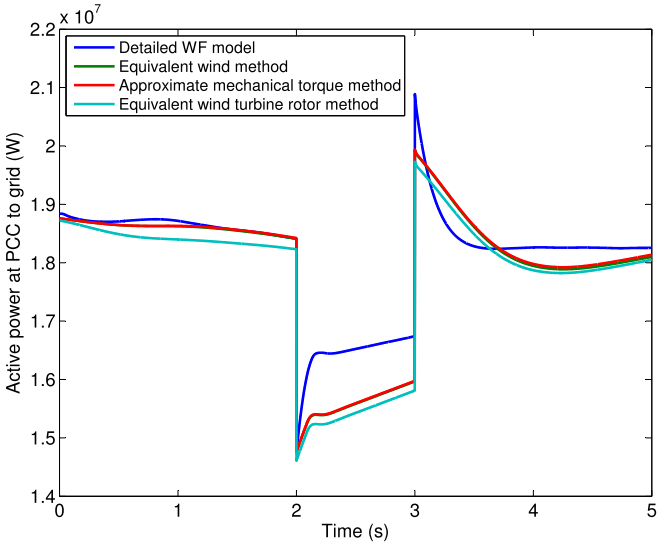

Fig. 13. Comparison of active power at PCC to grid generated by the detailed model and the three developed equivalent models when a slow voltage dip occurs.

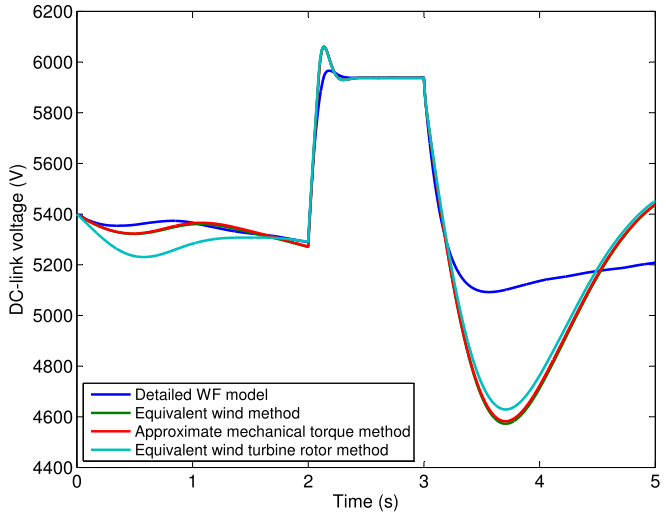

Fig. 14. Comparison of DC-link voltage generated by the detailed model and the three developed equivalent models when a slow voltage dip occurs.

Table 7
Comparison of the distance between the AWF models and the detailed model when a slow voltage dip occurs.

Average distance when a slow voltage dip occurs (%)			
Variable	Equiv. wind	Approx. T_m	EWT rotor
Active power at PCC to grid	0.243	0.236	0.343
DC-link voltage	0.134	0.128	0.114

operators require that WTs comply with a number of requirements to be able to respond to voltage dips. For instance, in Spain, *Red Eléctrica Española (REE)* has developed specific *Operational Procedures* to guarantee the system stability and security with a high wind power penetration. Specifically, the operational procedure P.O.12.3 sets the requirements of the wind systems response against voltage dips [33].

In variable speed PMSG WTs, the advantage of using a full scale power converter is the capacitor decoupling between the generator and the grid, what allows a full controllability of the system [34,35], and makes that the generator dynamic behaviour be not affected by grid faults.

The considered WF is studied under two types of dips:

- Slow dip: Voltage dip of long duration (1 s), where the voltage value falls to 0.8 p.u.
- Quick dip: Sharp drop in voltage, reaching 0.5 p.u. and lasting 0.5 s.

In this case, the incoming winds are given by test 1.

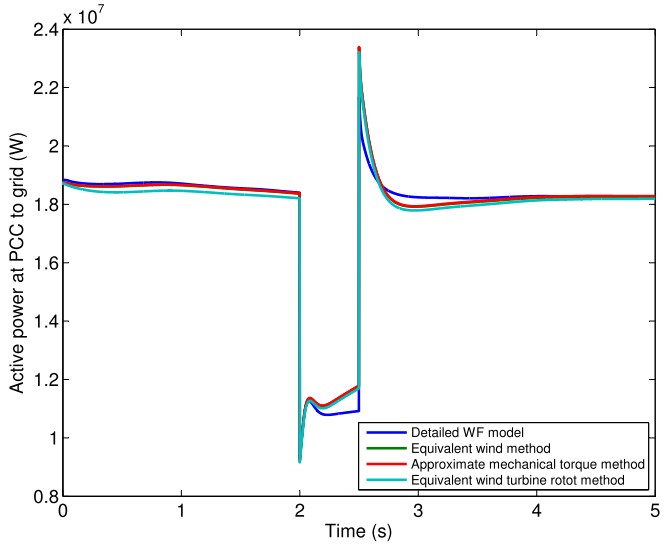

Fig. 15. Comparison of active power at PCC to grid generated by the detailed model and the three developed equivalent models when a quick voltage dip occurs.

4.3.1. Slow voltage dip

As shown in Fig. 13, the active power transmitted into the grid is proportional to the voltage existing at PCC, without showing significant transients during the disturbance. Moreover, as it can be seen, the responses of the AWF models are really similar to the detailed model response, although some small differences in the active power values respect to the detailed model can be appreciated when the fault occurs and when it is cleared.

The reason of these inequalities is the tuning of the grid-side converter controller. The equivalent grid-side converter PI has been tuned differently to the individual grid-side converter controllers due to the electrical system are aggregated in the AWF models. As the response speed is directly related to the parameters of the grid-side converter controllers, it has been necessary to reach a compromise between speed and stability of the DC-link voltage to determine these controller parameters of the AWF models. As shown in Fig. 13, the responses of the AWF models do not reach steady state at the fault clearance instant but this disadvantage allows the DC-link voltage not to reach a value excessively lower than its rated one when the fault is cleared, as shown in Fig. 14.

Furthermore, as discussed in Refs. [14,15], a braking resistor must be used to avoid overloading the DC-link capacitor when the voltage dip occurs, which could cause it to rupture. Then, when the DC-link voltage is over a certain limit (10% rated value), the braking resistor triggers and dissipates the excess energy stored in the capacitor, as depicted in Fig. 14, which avoids DC-link reaching an undesirable high value and facilitates the steady-state recovery.

As shown in Table 7, the distance values verify, once again, the similarity among the results, being the greatest distance between the model with *equivalent turbine rotor* method and the detailed model, in the case of active power, with a value slightly greater than 0.3%. And in the case of DC-link voltage, the distance between the three aggregated models and the detailed one is around 0.13%. So it can be concluded that the AWF models represent in a good way the active power and the DC-link voltage evolution during the slow voltage dip experienced by the studied WF.

4.3.2. Quick voltage dip

Figs. 15 and 16 show that the results of the AWF models are even more similar to the detailed model response when a quick voltage dip occurs than in case of a slow voltage dip, since the active power exchanged with the grid returns to the steady-state at the same instant in which the fault is cleared.

In this case, as it can be observed in Table 8, the distance values for the three AWF models are negligible and, therefore, it is clear that the responses of the developed AWF models are also excellent during the quick voltage dip experienced by the studied WF. The greatest value in average distance is that which corresponds to the model with *equivalent wind turbine rotor* method, with a value of 0.11%, when evaluating the active power. As for the DC-link voltage, the distance between the three equivalent models and the detailed model is 0.036%.

In relation to the computational time, as shown in Table 9, the best time reduction is about 19% for the *equivalent wind* method

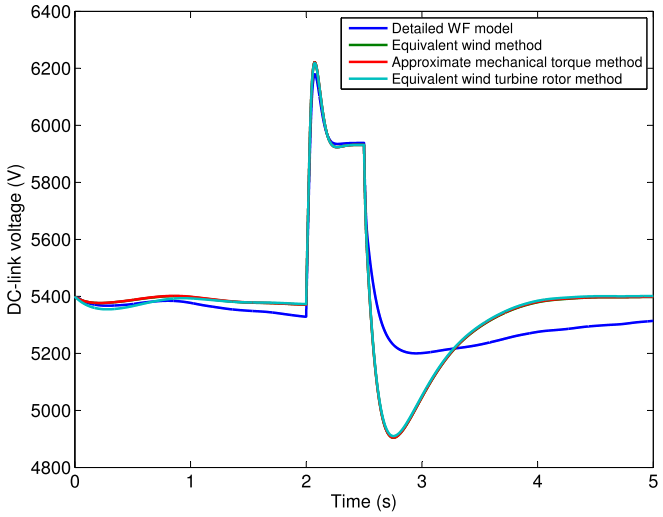

Fig. 16. Comparison of DC-link voltage generated by the detailed model and the three developed equivalent models when a quick voltage dip occurs.

Table 8
Comparison of the distance between the AWF models and the detailed model when a quick voltage dip occurs.

Average distance when a quick voltage dip occurs (%)			
Variable	Equiv. wind	Approx. T_m	EWT rotor
Active power at PCC to grid	0.089	0.087	0.110
DC-link voltage	0.036	0.036	0.036

with respect to the detailed model when a slow voltage dip occurs, being the best time reduction nearly 20% for the *equivalent wind turbine rotor* method with respect to the detailed model when a quick voltage dip occurs.

5. Conclusions

In this paper, using the aggregation methods proposed in existing literature on WTs with DFIG, three equivalent models of variable speed PMSG WFs have been developed for dynamic electrical studies: *equivalent wind*, *approximate mechanical torque* and *equivalent wind turbine rotor*.

In order to validate the effectiveness of the developed equivalent models to reproduce the behaviour of the WF during normal operation, two time series of wind speed have been introduced into the models, and time series of active power have been obtained as output. After analysing the results, it can be concluded that when the WF operates below nominal conditions, the three aggregation methods responses are virtually identical to the detailed model one, being the average distance between each aggregate model and that of the detailed model less than 0.02% in all cases.

On the other hand, when the WF operates at nominal conditions, the results of the aggregated model with *equivalent wind* and the one with *equivalent wind turbine rotor* are displaced with respect to the detailed model, being the results of the aggregated model with *approximate mechanical torque* virtually identical to the detailed one.

Moreover, to check the ability of the developed equivalent models to simulate the studied WF response when a voltage dip occurs at PCC, two voltage dips have been introduced into the models, getting to the output time series of active power and DC-link voltage to analyse the behaviour of the equivalent power converter during the grid disturbance. When a slow voltage dip occurs, the results of the three developed equivalent models are very similar to that of the detailed model, both in the evolution of the active power exchanged between the studied WF and the grid, and the evolution of the DC-link voltage.

When a quick voltage dip occurs, the results of the equivalent models are even more similar to the detailed model than in the previous voltage dip, since the active power exchange with the network returns to its nominal value almost immediately after the fault is fixed. In this case, the greatest value in average distance is that of the model with *equivalent wind turbine rotor*.

Concerning the computational time, the *equivalent wind turbine rotor* method provides the best time reductions with respect to the detailed model both for wind fluctuations (17%) and voltage dips (20%).

In short, it can be concluded that the three equivalent models provide very similar results to the detailed model, both in the evolution of active power when fluctuations in wind speed occur, and in the active power and DC-link voltage during the two voltage dips in the studied WF, as well as, a time reduction of 17% for the wind farm models according to the *equivalent wind turbine rotor* method for the wind fluctuations and a time reduction about 20% for the wind farm models according to the same aggregation method for the grid disturbances. Remarkably, the aggregated model with an *approximate mechanical torque* offers excellent results.

Acknowledgements

We are grateful to the anonymous reviewers who have contributed to improve the original manuscript.

Appendix A. PMSG wind turbine model equations

The mechanical power extracted from the wind by the wind turbine rotor can be expressed as follows [21],

$$P_w = \frac{1}{2}\cdot\rho\cdot\pi\cdot R^2\cdot C_p(\beta,\lambda)\cdot V_w^3, \tag{A.1}$$

where P_w is the mechanical power, ρ is the air density, R is the turbine rotor radius, C_p is the power coefficient and V_w is the wind speed.

The drive train is represented by the one-mass model and it is defined by the following equation [16], [29]:

$$T_m - Te = J_{eq}\cdot\frac{dW_r}{dt}, \tag{A.2}$$

Table 9
Comparison of time reductions for the studied aggregation methods when a voltage dip occurs.

Simulation time	Slow V. dip (s)	Reduction (%)	Quick V. dip (s)	Reduction (%)
Detailed model	242.0200		244.3600	
EW method	197.2538	**18.50**	200.3248	18.02
AMT method	213.5724	11.75	209.4928	14.27
EWT method	201.1679	16.88	197.3893	**19.22**

Figures in bold show the best time reduction for the different voltage dips.

where T_m is the mechanical torque, T_e is the electrical torque, J_{eq} is the equivalent inertia of the rotating system and W_r is the rotor angular speed.

The dynamic model of the PMSG has been built in the $d-q$ reference frame and it has the following form [21]:

$$u_{sd} = -R_s \cdot i_{sd} - L_{sd} \cdot \frac{di_{sd}}{dt} + W_e \cdot L_{sq} \cdot i_{sq} \quad (A.3)$$

$$u_{sq} = -R_s \cdot i_{sq} - L_{sq} \cdot \frac{di_{sq}}{dt} + W_e \cdot (\Psi_m - L_{sd} \cdot i_{sd}) \quad (A.4)$$

where u_{sd}, u_{sq} are the generator voltages, i_{sd}, i_{sq}, are the generator currents, R_s is the stator winding resistance, L_{sd}, L_{sq} are the stator inductances, Ψ_m is the magnet flux and W_e is the generator angular speed.

The DC-link model is defined by the following equation [29]:

$$\frac{du_{dc}}{dt} = \frac{1}{C} \cdot (I_{dc-R} - I_{dc-I}), \quad (A.5)$$

where u_{dc} is the DC-link voltage, C is the value of the DC-link capacitor, I_{dc-R} is the rectifier current and I_{dc-I} is the inverter current.

The dynamic model of the grid connection is the following [21]:

$$u_{gd} = u_{cd} - R_g \cdot i_{gd} - L_{gd} \cdot \frac{di_{gd}}{dt} + W_g \cdot L_{gq} \cdot i_{gq} \quad (A.6)$$

$$u_{gq} = u_{cq} - R_g \cdot i_{gq} - L_{gq} \cdot \frac{di_{gq}}{dt} - W_e \cdot L_{gd} \cdot i_{gd} \quad (A.7)$$

where u_{gd}, u_{gq} are the grid voltages, u_{cd}, u_{cq} are the voltages components of grid side converter, i_{gd}, i_{gq}, are the grid currents, R_g is the grid resistance, L_{gd}, L_{gq} are the grid inductances and W_g is the grid frequency.

Appendix B. Wind turbines and wind farm parameters

Table B.10. Wind turbine rotor parameters.

Wind turbine rotor		
Parameter		Value
Rated power (MW)		5
Diameter (m)		126
Equivalent inertia (Kg m^2)		$25.3 \cdot 10^6$
Power coefficient	C_1	0.5
	C_2	116
	C_3	0.5
	C_4	0
	C_5	5
	C_6	21

Table B.11. Electrical generator parameters.

Electrical generator	
Parameter	Value
Nominal power (MW)	5
Nominal voltage (kV)	3
Poles number	200
Frequency (rad/s)	$2\pi 50$
Stator resistance (mΩ)	1.8
Stator inductance (mH)	1.8
Magnetic flux (Wb)	3

Table B.12. Frequency converter parameters.

Frequency converter	
Parameter	Value
DC-link voltage (V)	5400
DC-link capacitor (mF)	14

Table B.13. PI controller parameters.

Parameter	Kp	Ki
PI controllers of individual WTs		
PI_{isd}, PI_{isq}	0.214 Ω	0.18 Ω/s
PI_{Pe}	2.52 e^{-4} A s	0.05 A
PI_{igd}, PI_{igq}	0.13 Ω	1.3 Ω/s
PI_{Udc}	−16.8 Ω^{-1}	−420 (Ω s)$^{-1}$
PI_{We}	100	200
PI controllers of equivalent WT		
PI_{isd}, PI_{isq}	0.214 Ω	0.18 Ω/s
PI_{Pe}	$7e^{-6}$ A s	$7e^{-3}$ A
PI_{igd}, PI_{igq}	0.044 Ω	0.44 Ω/s
PI_{Udc}	−9.84 Ω^{-1}	−196.8 (Ω s)$^{-1}$
PI_{We}	100	200

Table B.14. Internal grid parameters.

Internal grid	
Parameter	Value
Resistance (mΩ)	3.3
Inductance (mH)	0.13

Table B.15. 3/66 kV transformer.

3/66 kV transformer	
Parameter	Value
S_T (MVA)	40
ε_{cc} (%)	8

Table B.16. External grid parameters.

External grid	
Parameter	Value
Short circuit power (MVA)	500
X/R ratio	20

References

[1] World Wind Energy Association. 2013, half-year report. Tech. rep. World Wind Energy Association; 2013.

[2] Red Eléctrica de España. El sistema eléctrico español. Avance del informe 2013. Tech. rep. España: Red Eléctrica de España; 2013.

[3] Akhmatov V, Knudsen H. An aggregated model of a grid-connected, large-scale, offshore wind farm for power stability investigations – importance of windmill mechanical system. Electr Power Energy Syst 2002;24:709–17. http://dx.doi.org/10.1016/S0142-0615(01)00089-8.

[4] García CA. Modelos equivalentes de parques eólicos con aerogeneradores diferentes. Ph.D. thesis. University of Cadiz; 2008.

[5] Li H, Chen Z. Overview of different wind generator system and their comparisons. IET Renew Power Gener 2008;2(2):123–38. http://dx.doi.org/10.1049/iet-rpg:20070044.

[6] Akhmatov V. An aggregated model of a large wind farm with variable-speed wind turbines equipped with doubly-fed induction generators. Wind Eng 2004;28(4):479–86. http://dx.doi.org/10.1260/0309524042886423.

[7] Tapia G, Tapia A, Ostolaza JX. Two alternative modeling approaches for the evaluation of wind farm active and reactive power performances. IEEE Trans Energy Convers 2006;21(4):909–19. http://dx.doi.org/10.1109/TEC.2005.859975.

[8] Ali Muhammad, Milanovic JV, Ilie Irinel-Sorin, Chicco Gianfranco. Comparison of wind farm aggregate models for transient stability studies. In: 17th power systems computation conference, Stockholm, Sweden; 2011.
[9] Fernández L. Modelos multimáquina de aerogeneradores en parques eólicos. Ph.D. thesis. University of Cádiz; 2003.
[10] Fernandez LM, García CA, Sáez JR, Jurado F. Equivalent models of wind farms by using aggregated wind turbines and equivalent winds. Energy Convers Manag 2009;50(3):691–704. http://dx.doi.org/10.1016/j.enconman.2008.10.005.
[11] Poller M, Achilles S. Aggregated wind park model for analyzing power system dynamics. In: 4th international workshop on large-scale integration of wind power and transmission networks for offshore wind farms, Billund, Denmark; 2003.
[12] Fernandez LM, Jurado F, Sáez JR. Aggregated dynamic model for wind farm with doubly fed induction generator wind turbines. Renew Energy 2008;33(1):129–40. http://dx.doi.org/10.1016/j.renene.2007.01.010.
[13] Tande JOG. Final technical report. Dynamic model of wind farm for power system studies. Tech. rep. IEA Wind; 2007.
[14] Mercado-Vargas MJ, Deng Fujin, Rabaza O, Alameda-Hernandez E, Chen Zhe. Two control strategies for aggregated wind turbine model with permanent magnet synchronous generator. In: International conference on renewable energies and power quality – ICREPQ'12; 2012.
[15] Mercado-Vargas MJ. Modelos equivalentes de parques eólicos con generadores síncronos de imanes permanentes. Ph.D. thesis. University of Granada; 2012., http://hdl.handle.net/10481/23778.
[16] Slootweg JG, de Haan SWH, Polinder H, Kling WL. General model for representing variable speed wind turbines in power system dynamics simulations. IEEE Trans Power Syst 2003;18(1):144–51. http://dx.doi.org/10.1109/TPWRS.2002.807113.
[17] Fernandez LM, Garcia CA, Jurado F. Operating capability as PQ/PV node of a direct-drive wind turbine based on a permanent magnet synchronous generator. Renew Energy 2010;35:1308–18. http://dx.doi.org/10.1016/j.renene.2009.11.046.
[18] Buehring IK, Freris LL. Control policies for wind-energy conversion systems. IEE Proc Gen Trans Distr 1981;128(5):253–61.
[19] Ying M, Li G, Zhou M, Zhao C. Modeling of the wind turbine with permanent magnet synchronous generator for integration. In: IEEE power engineering society general meeting (PES 2007), Tampa, FL, E.E.U.U; 2007.
[20] Zaragoza J, Pou J, Arias A, Spiteri C, Robles E, Ceballos S. Study and experimental verification of control tuning strategies in a variable speed wind energy conversion system. Renew Energy 2011;36(5):1421–30. http://dx.doi.org/10.1016/j.renene.2010.11.002.
[21] Chinchilla M, Arnaltes S, Burgos JC. Control of permanent-magnet generators applied to variable-speed wind-energy systems connected to the grid. IEEE Trans Energy Convers 2006;21(1):130–5. http://dx.doi.org/10.1109/TEC.2005.853735.
[22] Belhadj J, Roboam X. Investigations of different methods to control a small variable-speed wind turbine with PMSM drives. J Energy Resour Technol 2007;129(3):200–13. http://dx.doi.org/10.1115/1.2748813.
[23] Ramtharan G, Jenkins N. Modelling and control of synchronous generators for wide-range variable-speed wind turbines. Wind Energy 2007;10(3):231–46. http://dx.doi.org/10.1002/we.219.
[24] Conroy JF, Watson R. Low-voltage ride-through of a full converter wind turbine with permanent magnet generator. IET Renew Power Gener 2007;1(3):182–9. http://dx.doi.org/10.1049/iet-rpg:20070033.
[25] Muyeen SM, Takahashi R, Murata T, Tamura J, Ali MH. Transient stability analysis of permanent magnet variable speed synchronous wind generator. In: Proc. of international conference on electrical machines and systems 2007., Seoul, Corea; 2007. http://dx.doi.org/10.1109/ICEMS.2007.4412242.
[26] Mercado-Vargas MJ, Gómez-Lorente D, Rabaza O, Alameda-Hernandez E. Comparison of control strategies of wind turbines with permanent magnet synchronous generator. Int Rev Model Simul. – IREMOS 2012;5(2):945–52.
[27] Rodriguez Amenedo JL, Burgos Diaz JC, Arnalte Gómez S. Sistemas eólicos de producción de energía eléctrica. Editorial Rueda, S.L.; 2003.
[28] Slootweg JG, Kling WL. Aggregated modelling of wind parks in power system dynamics simulations. In: IEEE power tech conference proceedings, vol. 3; 2003. http://dx.doi.org/10.1109/PTC.2003.1304458.
[29] Akhmatov V. Analysis of dynamic behaviour of electric power system with large amount of wind power. Ph.D. thesis. Technical University of Denmark; 2003.
[30] Manwell James, McGowan Jon, Rogers Anthony. Wind energy explained: theory, design and application. John Wiley & Sons Ltd.; 2009.
[31] Ackermann T, editor. Wind power in power systems. John Wiley & Sons Ltd.; 2005.
[32] Slootweg JG. Modelling and impact on power system dynamics. Ph.D. thesis. Technical University of Delft; 2003.
[33] Red Eléctrica de España. P.O. 12.3: Requisitos de respuesta frente a huecos de tensión de la instalaciones eólicas. Tech. rep. España: Eléctrica de España; 2006.
[34] Chen Z, Guerrero JM, Blaabjerg F. A review of the state of the art of power electronics. IEEE Trans Power Electron 2009;24(8):1859–75. http://dx.doi.org/10.1109/TPEL.2009.2017082.
[35] Blaabjerg F, Iov F, Chen Z, Ma K. Power electronics and control for wind power systems. In: 2010 IEEE international energy conference and exhibition, EnergyCon 2010, Manama, Bahrein; 2010. http://dx.doi.org/10.1109/ENERGYCON.2010.5771701.